JOURNAL OF CATALYSIS 81, 281–290 (1983)

An Experimental Method for Determining Heat of Physical Adsorption

DENNIS J. MILLER AND HONG H. LEE

Department of Chemical Engineering, University of Florida, Gainesville, Florida 32611

Received April 22, 1982

A new experimental method is presented for the measurement of the heat of physical adsorption of gases. The method involves thermal desorption of a gas from the solid sample in continuous flow sorptometer. The theoretical development postulates a dynamic equilibrium between adsorbed and free gas at all times during the thermal desorption, allowing calculation of heat of adsorption for a wide range of experimental conditions. The heat of adsorption is calculated from a single experimental run, and is therefore a simpler and quicker way of finding the heat of adsorption than traditional experimental methods. The heat of adsorption for a number of gas–solid systems has been determined, using simple Langmuir kinetics in the dynamic equilibrium model. The functional dependence of heat of adsorption on surface coverage has also been found from the experiments. The results show good agreement with the calorimetrically determined literature values.

INTRODUCTION

The importance of physical adsorption as an analytical tool for determining the area and characteristics of solid surfaces has long been recognized. Much literature has been published, including books by Brunauer (*1*), Young and Crowell (*2*), and Ross and Olivier (*3*) which deal entirely with physisorption. Of the literature published, much has been written about the heat of adsorption of physisorbed gases. The heat of adsorption is of primary importance in characterizing the solid surface and the gas–solid interactions (*4, 5*). There are two types of methods for the experimental determination of the heat of adsorption, direct and indirect measurement.

The direct measurement of heat of adsorption is carried out in very sensitive calorimeters designed specifically for adsorption. The determination of heat of adsorption is difficult, because the amount of heat liberated in physical adsorption and the volume of gas adsorbed are both small. Calorimeters have been designed and constructed by Beebe (*6*), Kiselev (*7*), and Morrison (*8*), and used to determine heats of physisorption for many systems. Despite the very sensitive nature of the measurements, the results of these investigators have yielded very useful information about the dependence of heat of adsorption on temperature, surface coverage, and sample preparation. Their successes have made the determination of heat of adsorption by calorimetry the most reliable method to date. Reviews of the direct methods of measuring heats of adsorption are given in Chap. 9 of Crowell and Young (*2*) and by Holmes in Chap. 5 of Flood (*9*).

The calculation of the isosteric heat of adsorption from adsorption data is carried out in two ways. The calculation of the limiting isosteric heat as $\theta \rightarrow 0$ is done using gas solid chromatography, as described by Ross and Olivier (*3*, p. 93). This method calculates only a single value of the heat of adsorption, and requires each solid being studied to be packed in a column.

The second and traditional method for calculating the isosteric heat of physical adsorption is through the application of the Clausiurs–Clapeyron equation to adsorption isotherm data (*10, 11*). The process involves the generation of adsorption isotherms and application of the C–C equation to adjacent isotherms with similar tempera-

0021-9517/83 $3.00

tures. The calculation is straightforward but generation of adsorption isotherms for the purpose of determining the heat of adsorption is very time consuming.

This work presents a new experimental technique which allows the isosteric heat of adsorption to be calculated from a single experimental curve. The method involves the generation of the isobar (θ vs T) curve by the thermal desorption in a continuous flow sorptometer. The new method is much less time consuming than the existing experimental techniques, and calculates the heat of adsorption via the Clausius–Clapeyron equation applied to the simple model of the desorption kinetics.

The heat of adsorption calculated in this work can be used to predict adsorption behavior for certain gas–solid systems. The results are particularly useful for screening adsorbates for possible use in a method for determining fractional catalyst surface area (*12*) and predicting optimum conditions for application of the technique.

THEORY

The general kinetic expression for the transient adsorption–desorption on a free surface at submonolayer coverage is

$$V_m \frac{d\theta}{dt} = k_a p f(1 - \theta) - k_d g(\theta) \qquad (1)$$

where k_a = adsorption rate constant, k_d = desorption rate constant, p = partial pressure of adsorbate, V_m = monolayer volume of adsorbate per unit area, and θ = fractional coverage of surface. The functions $f(1 - \theta)$ and $g(\theta)$ represent the fraction of vacant and occupied sites, respectively.

The order of magnitude of the three terms in Eq. (1) can be calculated using collision theory for the adsorption rate, transition state theory for the desorption rate, and an estimate of the transient term from experiment. For carbon dioxide partrial pressure of 0.1 atmosphere and 300°C

$$r_a = k_a p f(1 - \theta) = 10^3\,\sigma f(1 - \theta)\ \text{moles/m}^2 \cdot \text{sec} \qquad (2)$$

$$r_d = k_d g(\theta) = \left[\begin{array}{l} 10^2 g(\theta)\ \text{moles/m}^2 \cdot \text{sec} \\ \qquad (E_d = 7\ \text{kcal/mole}) \\ 10^5 g(\theta)\ \text{moles/m}^2 \cdot \text{sec} \\ \qquad (E_d = 3\ \text{kcal/mole}) \end{array}\right. \qquad (3)$$

where E_a (adsorption activation energy) has been assumed to be zero and E_d is the desorption activation energy.

The transient term can be estimated by experimentally limiting the maximum value of $d\theta/dt$ to 1/min. For the desorption of a monolayer of carbon dioxide (area per molecule = 25 Å^2)

$$V_m \frac{d\theta}{dt} = 6 \times 10^{-6} \left(\frac{1}{60\ \text{sec}}\right) = 10^{-7}\ \text{moles/m}^2 \cdot \text{sec}. \qquad (4)$$

A comparison of the three terms shows that the transient term is much smaller than r_a and r_d except as θ approaches zero or unity. The kinetics of the thermal desorption are therefore adequately described by

$$k_a p f(1 - \theta) = k_d g(\theta) \qquad (5)$$

which states that a dynamic equilibrium is maintained at all times between adsorption and desorption. The existence of the dynamic equilibrium can also be illustrated by solving Eq. (1) if $f(1 - \theta) = 1 - \theta$ and $g(\theta) = \theta$, and noting the rapid decay of the transient term. The concept of rapid dynamic equilibrium has also been studied by Brunauer (*1*, p. 460).

Equation (5) states that the value of θ is only a function of the instantaneous pressure and temperature of the system. For the experimental conditions encountered in the continuous flow sorptometer during thermal desorption, the adsorbate partial pressure over the solid sample remains essentially constant. The calculations which support this claim are presented in Appendix I for typical sorptometer conditions. With constant partial pressure, the value of θ at any point during the thermal desorption is a function only of the system temperature. Experiments carried out in our laboratory at different heating rates yielded the same curve of coverage versus temperature. Furthermore, the equilibrium values of θ at constant T and P (obtained by step changes in temperatures), were very similar to the values at the same temperature from thermal desorption. This similarity is shown in Fig. 1. These two experiments verify the postulates of the dynamic equilibrium.

When the rate constants k_a and k_d are expressed as a function of temperature in Eq. (5), the resulting expression can be rearranged and the logarithm taken to yield

$$\ln\left(\frac{k_{a0}P}{k_{d0}}\right) + \ln\frac{f(1-\theta)}{g(\theta)T^{1/2}} = \frac{-\Delta H_a(\theta)}{RT} \qquad (6)$$

where $H_a(\theta) = E_d - E_a$ is the heat of adsorption. Application of the Clausius–Clapeyron equation to Eq. (6) shows that $\Delta H(\theta)$ is the isosteric heat of adsorption.

Before Eq. (6) can be applied to experimental data, the functional forms of $f(1 - \theta)$ and $g(\theta)$ must be assigned. The physical adsorption of gases such as nitrogen or carbon dioxide is nondissociative at near-liquefaction temperatures. The adsorption onto an empty surface is preferred over that onto an adsorbed molecule, because interactive forces are largest between adsorbent and adsorbate. Because the present work focuses on the calculation of the heat of adsorption and its subsequent application and not the fundamental nature of the adsorbent–adsorbate interactions, the functional forms $f(\theta) = 1 - \theta$ and $g(\theta) = \theta$ will be used in this work. These forms are by far the most widely used in practice; the use of other forms such as θ^2 and $(1 - \theta)^2$ cannot be justified for low partial pressure physical adsorption without further, in-depth study of adsorption behavior. It should be noted however, that the heat of adsorption can be calculated from Eq. (6) for any form of f and g as long as the dynamic equilibrium is seen to hold from Eqs. (2)–(4).

The rigorous development of Eq. (6) from kinetic theory or statistical mechanics requires stringent assumptions. Of concern here are the assumptions of no adsorbate–adsorbate interactions and an energetically homogeneous surface, which are seldom seen in reality. The usual way of accounting for surface heterogeneity and adsorbate interactions is to treat Eq. (6) not as rigorous but as a semiempirical model, and to assign

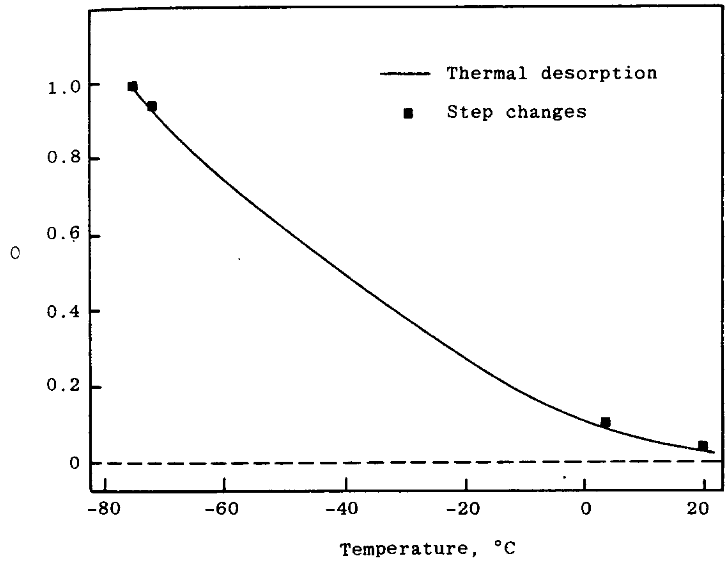

FIG. 1. Comparison of equilibrium values of θ with those found from thermal desorption at constant partial pressure.

a functional form to $\Delta H(\theta)$. Any functional form of $\Delta H(\theta)$ can be used which fits the experimental data. The Tempkin isotherm is derived using the linear functional form of $\Delta H(\theta)$

$$\Delta H(\theta) = \Delta H_0(1 - \alpha\theta). \qquad (7)$$

This functional form will be seen to hold over fairly wide ranges of θ for all gas–solid systems studied in this work.

Insertion of Eq. (7) into (6) allows the dependence of $\Delta H(\theta)$ on θ to be determined from the isobar generated from thermal desorption

$$\ln\left(\frac{k_{a0}p}{k_{d0}}\right) + \ln\left(\frac{1-\theta}{\theta T^{1/2}}\right) - \frac{\alpha\Delta H_0\theta}{RT} = \frac{-\Delta H_0}{RT}. \qquad (8)$$

The parameters α and ΔH_0 are determined by first doing a least square fit to find the value of $\alpha\Delta H_0/R$ which gives the straightest line of the plot of $[\ln(1 - \theta/\theta T^{1/2}) - \alpha\Delta H_0\theta/RT]$ vs $1/T$ from the experimental θ vs T data. The slope of the best line is $-\Delta H_0/R$, which then allows α to be found from the term $\alpha\Delta H_0$. The intercept of the line is $\ln(k_{a0}/p/k_{d0})$. These computations have been performed on a computer.

APPARATUS, PROCEDURE, AND DATA REDUCTION

The experimental equipment consists of a Perkin–Elmer continuous flow sorptometer which has been modified for thermal desorption studies. A schematic of the apparatus is given in Fig. 2. The carrier gas used in these experiments is helium (Airco Grade 5, 99.999%), the adsorbates are nitrogen (Airco Grade 5, 99.999%), ethylene (Matheson, 99.98%), and carbon dioxide (Airco Grade 4, 99.99%).

The sample cell used in the experiments consists of two vertical concentric Pyrex tubes joined by a ground glass fitting, as shown in Fig. 3. The sample forms a shallow bed approximately 1 cm in diameter and 0.3 cm in depth, over which the gas flows. The temperature at two places in the bed is continuously monitored by two thermocouples.

Equation (9) was developed using two assumptions concerning the solid sample: the sample temperature is uniform everywhere in the sample bed, and the partial pressure over the solid surface is uniform, i.e., there is no diffusion resistance within the particles or within the bed.

The use of two thermocouples in the sample bed allowed the temperature gradi-

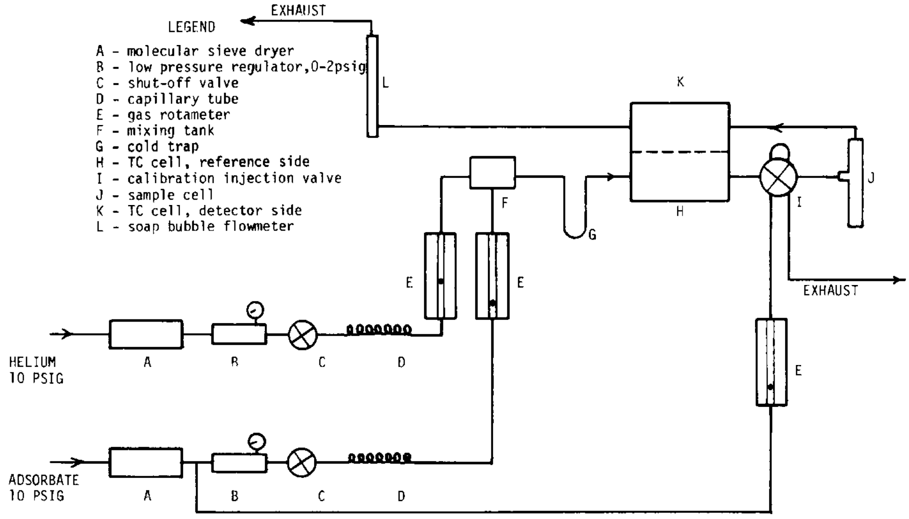

FIG. 2. Schematic diagram of sorptometer.

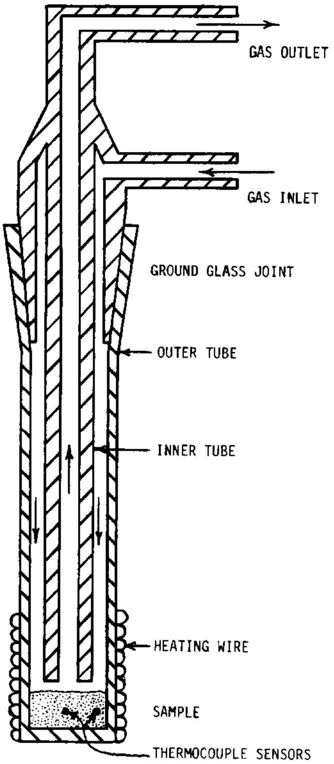

FIG. 3. Cutaway view of sample cell.

ent to be estimated. The maximum temperature difference from the outside to the center of the bed was found to be between 5° and 10°C at the maximum heating rate for all samples studied. While not insignificant, this nonisothermality does not prevent the application of Eq. (6), and is taken into account by using the average of the two temperatures in the calculations. The temperature difference is minimized by using the lowest possible heating rate during thermal desorption.

The presence of diffusional resistances within the bed is minimized by careful choice of the solid sample structure. Intraparticle diffusion has been virtually eliminated by using nonporous particles of solid sample in the experiments. The total surface areas of the solid samples ranged from 0.3 to 20 m^2/g. This surface area, measured by BET method, corresponds closely to the external surface area calculated from the particle size. The interparticle diffusion is minimized by using low heating rates and a shallow sample bed. The degree of diffusion is calculated in Appendix II for a step change in the bed gas concentration.

The experimental procedure and the analysis of data used to obtain the θ vs T curve, as well as a more thorough description of the apparatus, are described in detail elsewhere (*12*). The experimental procedure consists of recording the sample temperature and volume of gas desorbed as a function of time during the thermal desorption. Because the volume adsorbed is a function only of temperature, the sample can be heated in any manner for collection of the data. The monolayer volume used to calculate θ is determined from an independent BET experiment using the same adsorbate.

RESULTS

The thermal desorption experiments have been carried out for the gas–solid pairs listed in Table 1. The sorptometer was run at a total pressure of 1 atm. and a total flow rate of 35 ml/min. The thermal desorption took place over a period of 2–3 min.

The θ vs T curves for the gas–solid pairs are given in Figs. 4–6 for the three adsorbates used. The calculated values of ΔH_0, α, and k_{d0}/k_{a0} are given in Table 2, along with the range of θ for which the θ vs T data can be fitted to Eq. (8). This range was determined to be the points where a value of θ calculated from Eq. (8) differed from the experimental value by more than 3%.

DISCUSSION

The range of fractional surface coverage for which Eq. (8) can be applied is generally $0.1 < \theta < 0.6$. The dependence of heat of adsorption on surface coverage in this region is generally quite weak. This is typical behavior for physical adsorption. At low surface coverages, the deviation is due to the relatively small number of surface sites (edges, cracks, etc.) which have a relatively higher affinity for adsorbate. This increased

TABLE 1

Experimental Conditions

Gas	Solid	Adsorbate partial pressure (atm)	Initial fractional coverage	Minimum temperature of adsorption (°C)
N_2	Carbon black[a]	0.082	0.96	−195
N_2	K_2CO_3[b]	0.082	0.98	−195
CO_2	Carbon black	0.105	0.32	−78.5
CO_2	K_2CO_3	0.105	0.60	−78.5
CO_2	Al_2O_3[c]	0.082	0.95	−78.5
CO_2	Pt powder[d]	0.082	0.79	−78.5
C_2H_4	Al_2O_3	0.141	0.95	−78.5
C_2H_4	Pt powder	0.141	0.872	−78.5

[a] Graphitized, $S = 21.7\ m^2/g$, Fisher Scientific.

[b] Ground to 325 mesh, anhydrous, $S = 0.7\ m^2/g$.

[c] Norton SA5202, $S = 1.0\ m^2/g$, ground to 200 mesh.

[d] Pfaltz & Bauer, $S = 0.6\ m^2/g$.

TABLE 2

Results–Heats of Adsorption $\Delta H(\theta) = \Delta H_0(1 - \alpha\theta)$

Gas	Solid	ΔH_0 (kcal/mole)	α	$\frac{k_{a0}}{k_{d0}}$ (°C$^{-1/2}$)	Range of fit
N_2	Carbon black	3.04	0.178	2320	$0.10 < \theta < 0.70$
N_2	K_2CO_3	3.29	0.238	5480	$0.16 < \theta < 0.64$
CO_2	Carbon black	4.86	0.027	3590	$0.05 < \theta < 0.31$
CO_2	K_2CO_3	6.35	0.165	8660	$0.05 < \theta < 0.58$
CO_2	Al_2O_3	4.85	0.042	206	$0.15 < \theta < 0.46$
CO_2	Pt	4.61	0.027	198	$0.18 < \theta < 0.63$
C_2H_4	Al_2O_3	4.62	0.013	253	$0.12 < \theta < 0.55$
C_2H_4	Pt	3.91	0.03	71	$0.12 < \theta < 0.50$

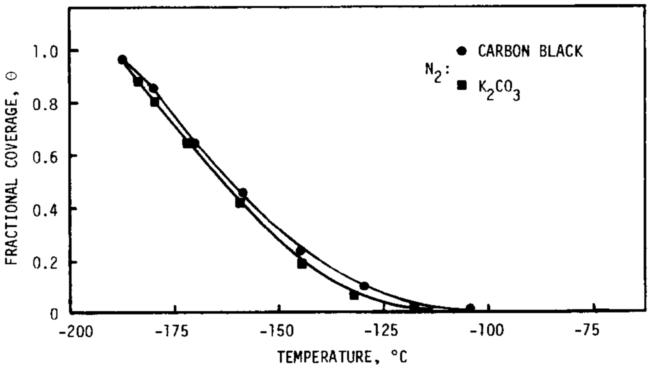

FIG. 4. Coverage vs temperature for N_2 thermal desorption.

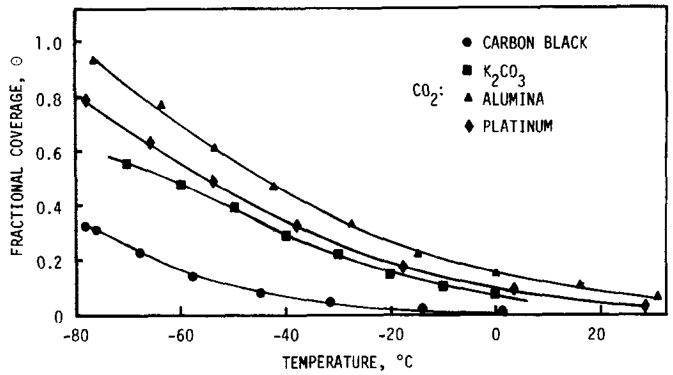

FIG. 5. Coverage vs temperature for CO_2 thermal desorption.

heat of adsorption results in a higher experimental value of θ than predicted by Eq. (8). This is shown in Fig. 7. At fractional coverage greater than 0.6, adsorbate–adsorbate interactions and the onset of multilayer formation are responsible for deviations from the model. These effects are seen as the increase in the experimental value of θ not predicted by Eq. (8).

The heat of adsorption calculated by Eq. (8) is the isosteric heat of adsorption. The comparison of the isosteric heats calculated with those measured by calorimetry requires recognition that the isosteric heat and the calorimeteric differential heat are two different quantities. A thorough treatment of this fact is presented by Ross and Olivier (*3*, p. 103), with the final result being

$$q_{\text{isosteric}} - RT = q_{\text{differential}}.$$

The two quantities differ by RT, which is of the order of 0.4 to 0.6 kcal/mole for the gas–solid pairs studied here. The comparison of the calculated heats of adsorption with values obtained from the literature is given in Table 3. The literature values have been determined both calorimetrically and from isotherm data. The comparison shows fairly good agreement of the heats of adsorption. It must be remembered that the heat of adsorption is a function of the solid surface, so comparison with different types of carbon or of K_2CO_3 with KCl must be made with caution.

The primary advantage of this method is that it allows calculation of the heat of adsorption from a single thermal desorption run. There is no need to develop a set of adsorption isotherms, or to use static methods to assure that equilibrium data are collected.

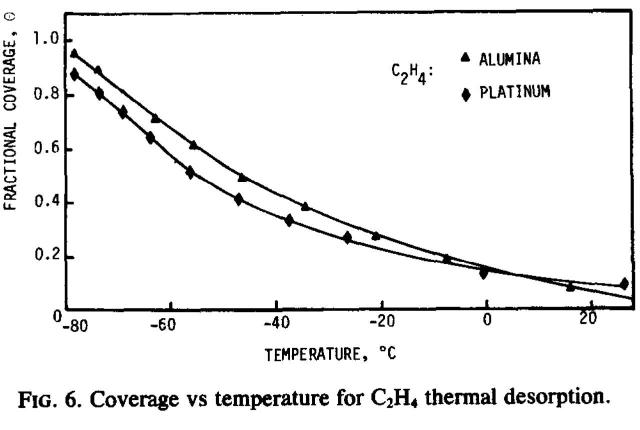

FIG. 6. Coverage vs temperature for C_2H_4 thermal desorption.

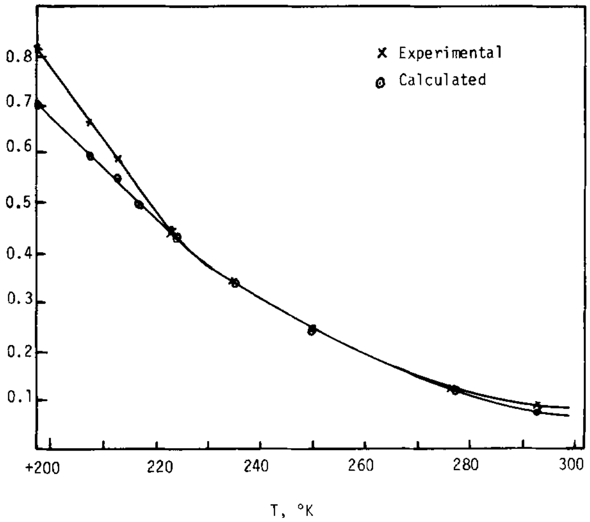

FIG. 7. Comparison of experimental θ vs T curve with that calculated from heat of adsorption for C_2H_4 on platinum.

CONCLUSONS

The heat of adsorption can be calculated as a function of θ from a single θ vs T experimental curve, using a linear dependence on θ. The experimental method yields fairly accurate heat of adsorption. The method provides a quick and simple way of estimating the heat of adsorption.

APPENDIX I

The sample cell and experiments have been designed to minimize changes in adsorbate partial pressure over the solid sample during thermal desorption.

The maximum rate of desorption will cause the largest change in adsorbate partial pressure in the sample cell. Of all experiments performed, thermal desorption of CO_2 from carbon over a period of 1 min gave the largest rate of desorption, equal to 0.18 ml/min.

The typical total flow rate and adsorbate partial pressure were 35 ml/min and 0.08

TABLE 3

Comparison of Results with Literature Values

Experimental results			Literature values			
Gas	Solid	$\Delta H_a \left(\frac{\text{kcal}}{\text{mole}}\right)$	Solid	$\Delta H_a \left(\frac{\text{kcal}}{\text{mole}}\right)$	Method of determination	Reference
N_2	Carbon black	$2.5(\theta \rightarrow 1)$ $3.04(\theta = 0)$	Graphon	$1.7(\theta = 1)$ $2.9(\theta \rightarrow 0)$	Calorimetry	(*4*, *5*)
			Sterling S&L	$2.0(\theta = 1)$ $3.8(\theta \rightarrow 0)$	Calorimetry	
N_2	K_2CO_3)	$2.8(\theta = 0.5)$ $3.3(\theta = 0)$	KCl	$2.4(\theta = 0.5)$ $3.0(\theta = 0)$	Clausius–Clapeyron equation	(*15*)
CO_2	Carbon black	$4.8(\theta \rightarrow 0)$	Carbon black	$4.3(\theta \rightarrow 0)$	Calorimetry	(*14*)
CO_2	K_2CO_3	$6.3(\theta = 0)$	KCl	6.4	Clausius–Clapeyron equation	(*16*)

atm., corresponding to an adsorbate flow of 2.8 ml/min. The sample cell volume is about 1 ml, so that the residence time of gas is of the order of 2 sec. For this continuous flushing, the adsorbate partial pressure increases to

$$\frac{2.8 + 0.18}{35 + 0.18} = 0.085 \text{ atm} \qquad \text{(AI-1)}$$

an increase of 6%. This change in partial pressure results in the value of θ predicted by the Langmuir isotherm to change by a maximum of 0.014 at $\theta = 0.5$. This deviation is within the experimental error for the thermal desorption experiment.

The majority of samples used in this study adsorbed only about 5–10% as much adsorbate as carbon over a longer time span, so the changes in partial pressure over the sample can be neglected in the experiments. The change in partial pressure is still great enough, however (>0.1%), to allow accurate detection by the thermal conductivity cell.

APPENDIX II

Appendix I showed that, in a well-mixed sense, the change in adsorbate partial pressure can be neglected in the solid sample. However, the question of concentration gradients within the bed of nonporous sample particles must be addressed to assure the existence of the macroscopic dynamic equilibrium.

The extent of diffusion resistance can be determined by examining the extreme case of all gas desorbing instantaneously from the solid sample. This instantaneous desorption is a result of a step change in temperature from the adsorption temperature T_a to a high temperature, and results in a step change in concentration of adsorbate in the sample bed at the instant of temperature change. If the relaxation or decay time of the step change in concentration is negligible compared to the time of a thermal desorption run, diffusion within the bed can be justifiably neglected.

The decay of the step change can be examined by solving the unsteady state diffusion equation for a one-dimensional solid. The dimensionless form of the equation is

$$\frac{\partial c}{\partial \tau} = \frac{\partial^2 c}{\partial z^2} \qquad \text{(AII-1)}$$

where $\tau = D_e t/L^2$, $z = x/L$, D_e = effective diffusivity of adsorbate in packed bed, and L = bed depth. The derivation of this equation and the boundary conditions for a step change in a finite slab are given in Carslaw and Jaeger (*13*, p. 101). The solution is given in graphical form for the step change in concentration. For a value of $\tau = 1.0$ sec, the concentration in the bottom of the sample bed (farthest from the gas stream) should decrease to only 10% of the magnitude of the step change above the bulk gas concentration. For values of $D_e = 0.1$ cm^2/sec and $L = 0.3$ cm (which are typical sample bed parameters), the value of $\tau = 1.0$ is reached in $t = 0.9$ seconds. Thus, about 95% of the gas desorbed during the instantaneous desorption has entered the gas stream after only 1 sec, signifying that the rate of diffusion is large. Because the rate of diffusion is much faster than the rate of thermal desorption, the effects of diffusion can be neglected in the thermal desorption. This has been observed experimentally by increasing and decreasing the sample temperature a few degrees and monitoring the thermal conductivity cell output. In all cases, rapid adsorption and desorption is observed in accordance with the temperature changes.

REFERENCES

1. Brunauer, S., "The Adsorption of Gases and Vapors—Physical Adsorption." Princeton Univ. Press, Princeton, N.J., 1943.

2. Young, D. M., and Crowell, A. D., "Physical Adsorption of Gases." Butterworths, London, 1962.

3. Ross, S., and Olivier, J. P., "On Physical Adsorption." Wiley–Interscience, New York, 1964.

4. Beebe, R. A., Biscoe, J., Smith, W. R., and Wendell, C. B., *J. Amer. Chem. Soc.* **69,** 95 (1947).

5. Beebe, R. A., Biscoe, J., Smith, W. R., and Wendell, C. B., *J. Amer. Chem. Soc.* **69,** 2294 (1947).

6. Amberg, C. H., Spencer, W. B., and Beebe, R. A., *Canad. J. Chem.* **33,** 305 (1955).

7. Dzhigit, O. M., Kiselev, A. V., and Muttik, G. G., *J. Phys. Chem.* **66,** 2127 (1962).

8. Morrison, J. A., and Los, J. M., *Discuss. Faraday Soc.* **8,** 321 (1950).

9. Holmes, J. M., *in* "The Gas–Solid Interface" (E. A. Flood, Ed.), Chap. 5. Dekker, New York, 1967.

10. Hasz, J. W., and Barrere, C. A., Jr., *AIChE Symp. Ser.* **65,** (96), 48 (1969).

11. Pace, E. L., Dennis, K. S., Greene, S. A., and Heric, E. L., *Canad. J. Chem.* **33,** 245 (1955).

12. Miller, D. J. Ph.D. thesis, Univ. of Florida Gainesville, 1982.

13. Carslaw, H. S., and J. C. Jaeger, "Conduction of Heat in Solids." Oxford Univ. Press, London, 1959.

14. Spencer, W. B., Amberg, C. H., and Beebe, R. A., *J. Phys. Chem.* **62,** 719 (1958).

15. Orr, W. J. C., *Proc. R. Soc. A* **173,** 349 (1939).

16. Hayakawa, T., *Bull. Chem. Soc. Jpn.* **30,** 332 (1957).